The Effects of Positioning of Transcatheter Aortic Valves on Fluid Dynamics of the Aortic Root

Elliott M. Groves,*† Ahmad Falahatpisheh,* Jimmy L. Su,*‡ and Arash Kheradvar*†‡

Transcatheter aortic valve implantation is a novel treatment for severe aortic valve stenosis. Due to the recent use of this technology and the procedural variability, there is very little data that quantify the hemodynamic consequences of variations in valve placement. Changes in aortic wall stresses and fluid retention in the sinuses of Valsalva can have a significant effect on the clinical response a patient has to the procedure. By comprehensively characterizing complex flow in the sinuses of Valsalva using digital particle image velocimetry and an advanced heart-flow simulator, various positions of a deployed transcatheter valve with respect to a bioprosthetic aortic valve (valve-in-valve) were tested *in vitro*. Displacements of the transcatheter valve were axial and directed below the simulated native valve annulus. It was determined that for both blood residence time and aortic Reynolds stresses, it is optimal to have the annulus of the transcatheter valve deployed as close to the aortic valve annulus as possible. *ASAIO Journal* 2014; 60:545–552.

Key Words: valve-in-valve, Reynolds stresses, aorta, transcatheter aortic valve replacement, valve placement

Calcific aortic stenosis (AS) is a common valvular heart pathology that has become increasingly more prevalent as the population has aged. Historically, AS patients required invasive open heart surgery that is not well tolerated by the older and more medically ill population. However, the option of transcatheter aortic valve replacement (TAVR) has transformed the treatment of aortic valve stenosis for high-surgical-risk patients who now have a lifeline, despite their age, comorbidities, or Society of Thoracic Surgeons' risk model score.[1,2]

As the indications for TAVR grow, increased attention is being paid to the long-term procedural implications. The effects of transcatheter valve positioning on aortic flow is an important characteristic of the procedure that has not been studied in detail. With an open surgical procedure, valve placement is precise; however, more variability is expected in TAVR due to the inherent nature of the procedure.[3] The most important consequences of variability in valve placement are impairment of flow to the coronary arteries and the alteration of valvular hemodynamics, which can affect ventricular performance, valve durability/function, and aortic wall strain.[4] Incorrect valve placement can lead to significant complications such as valve embolization and severe paravalvular leak.[4] Up to this point there has been no well-designed study to examine the hemodynamic effects of differing TAVR positions. Currently, the recommendation is that the commercially available transcatheter valves should be placed at or just below the native valve annulus[5]; however, this has never been quantitatively confirmed as an optimal position.[6] In addition, there is little data as to whether a more liberal positioning below the annulus would result in negative consequences.

Through a series of *in vitro* experiments, we recreated conditions mimicking a transcatheter aortic valve being implanted at several different axial positions with respect to the aortic valve annulus. Our goal was to determine whether the fluid dynamics of the aortic root and ascending aorta would be significantly altered with valve position at varying cardiac outputs. Measuring the particle residence time in the aortic root allows for a surrogate measure of coronary perfusion and potential for thrombus formation; an exceedingly long residence time can lead to thrombus formation in the sinus, whereas too short a residence time does not allow for proper coronary blood flow.[7] We also sought to characterize the flow in the proximal aorta to determine whether TAVR positioning may have deleterious long-term consequences on the flow in the ascending aorta.

Methods

As the systolic and diastolic phases of the cardiac cycle each takes place at sub-second time increments, a highly accurate modality with high temporal resolution is needed for imaging. Digital particle image velocimetry (DPIV) is a robust and validated technique for imaging, assessing, and quantifying cardiac fluid dynamics *in vitro*.[8–11] The high spatial and temporal resolution of DPIV allows for accurate assessment of cardiovascular devices such as heart valves under different conditions.[12–15] To utilize DPIV for cardiovascular device assessment, precise replication of cardiac flow fields *in vitro* is essential. An advanced cardiac flow simulator, as detailed below, was used for this study.

Experimental Setup

Pulsatile pump system. The heart-flow simulator consists of a hydraulic pump system (Superpump system, VSI, SPS3891;

From the *Edwards Lifesciences Center for Advanced Cardiovascular Technology, University of California at Irvine, Irvine, California; †Division of Cardiovascular Diseases, University of California at Irvine, Irvine, California; and ‡Department of Biomedical Engineering, University of California at Irvine, Irvine, California.

Submitted for consideration January 28, 2014; accepted for publication in revised form May 17, 2014.

The first two authors contributed equally to this work.

The authors have no conflicts of interest to report.

This work was partially supported by a Coulter Translational Research Award (CTRA) from the Wallace H. Coulter Foundation and by the National Center for Research Resources, the National Center for Advancing Translational Sciences, and National Institutes of Health, through grant UL1 TR000153.

Correspondence: Arash Kheradvar, Edwards Lifesciences Center for Advanced Cardiovascular Technology, University of California at Irvine, 2410 Engineering Hall, Irvine, CA 92697. Email: arashkh@uci.edu.

DOI: 10.1097/MAT.0000000000000107

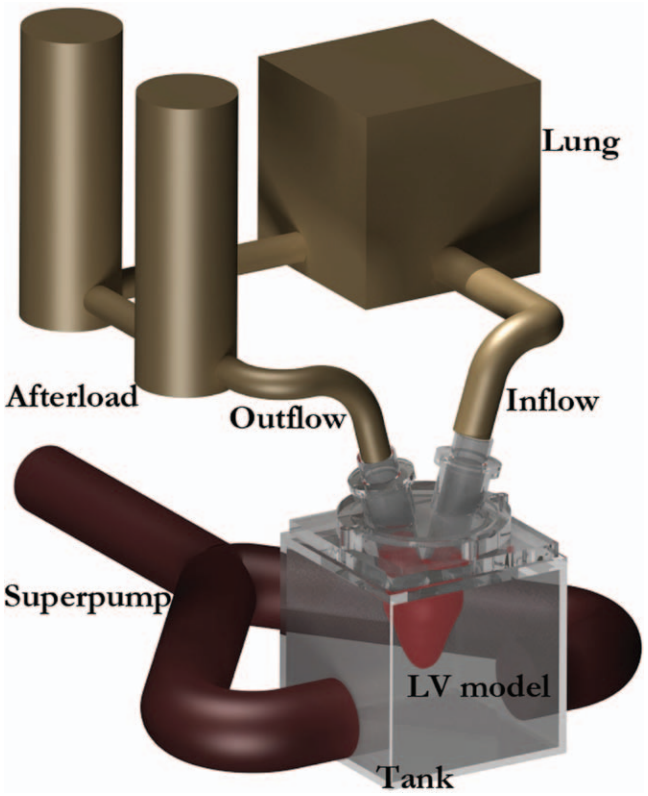

Figure 1. The heart-flow simulator schematic is illustrated, all components are included, and their functions are discussed in the text. LV, left ventricular. full color online

Vivitro Systems, Inc., Victoria, BC, Canada), which operates based on a VSI Wave Generator VG2001 (Vivitro Systems, Inc.).[16] The system is comprised of a silicone left ventricular (LV) sac custom-built mimicking the adult human LV suspended in a pressurized container. The schematic of the system is shown in **Figure 1**. The periodic, pulsatile flow in the circulatory system is generated as the response of the ventricular sac to the input waveforms supplied by the pump. The wave generator creates physiological waveforms that reproduce the desired systolic ratio (SR) of 35% for the LV model; SR is the fraction of time in a cardiac cycle that the LV is in systole. Particle-seeded water was used as the circulating fluid.

Aorta model. To accurately assess the dimensions of a human aorta, published data were used from prior pooled human echocardiographic studies to determine the proper dimensions.[17] It has been validated through direct surgical measurement that both computed tomography and echocardiographic data are accurate modalities to define human aortic dimensions.[18] Using these data, a computerized model was made, and an aortic model was constructed with acrylic plastic (Plexiglas) and then was used for this study. The root of the model is axially symmetric and represents a nonpathologic state. As seen with many patients with severe AS, the majority in fact do not have a pathologically dilated aorta.[19] **Figure 2A** shows the model used in the experiment.

Ventricular model. The geometry of the ventricle model is obtained from three-dimensional reconstruction of a normal adult heart using cardiac magnetic resonance imaging (MRI) in systolic state. The model is manufactured through dip-molding in transparent silicone. The LV model was assembled in the circulatory system through connecting to inlet and outlet tubes. The lengths of the tubes are adjustable to fit to a variety of ventricular models used for different experiments.

Artificial heart valves. A 25-mm bileaflet mechanical mitral valve was placed at the mitral position of the LV. For the aortic position, a fresh 29-mm Carpentier-Edwards Perimount bioprosthetic surgical aortic valve (Edwards Lifesciences, Irvine, CA) was used. The selection of a larger bioprosthetic valve was made to accommodate the transcatheter valve used to ensure full expansion of the stent.[20] Allowing for full stent expansion provides the truest representation of hemodynamics. This experimental setup was used to obtain baseline data. For the transcatheter aortic valve, a 25-mm Nitinol stented valve with bovine pericardial leaflets (FOLDAVALVE; Folda LLC, Mission Viejo, CA), which shares many characteristics with the currently available transcatheter valves, was placed at different positions with respect to the mock-up aortic root within the bioprosthetic aortic valve (valve-in-valve). The transcatheter valve's annulus was placed at 5, 10, 15, and 20 mm below the aortic annulus in the simulator. Each position was tested at 2 and 4 L/min of cardiac output, which at 60 bpm correlate to a stroke volume of 33 and 66 ml, respectively. The experiments were then repeated with a new transcatheter valve of the same type to ensure reproducibility.

DPIV setup. Neutrally buoyant (Rhodamine B) particles with a diameter of 15 μm (Fluostar; Kanomax, Inc., Andover,

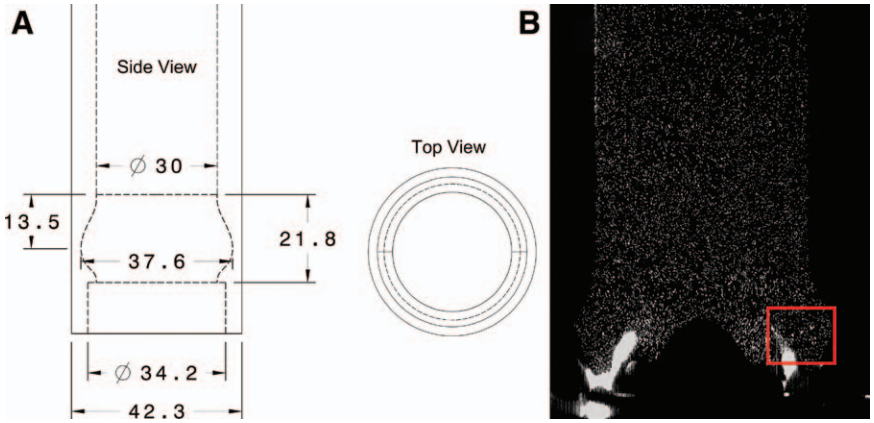

Figure 2. A: Geometry of the aortic model (side and top views). **B**: The aortic model with the presence of particle image velocimetry (PIV) particles during the experimental analysis. The region of interest used for calculating particle residence time is highlighted by a red box. full color online

NJ) were used for seeding the flow. A single high-speed digital camera (1,000 frames per second, 1,280×1,024; Y3, IDTVision, Inc. Pasadena, CA) was positioned to capture the image sequences of the particle fields illuminated by an Nd:YLF green pump laser (Evolution 30; Coherent, Inc., Santa Clara, CA) with the beam crossing two valve leaflets. The pair of images were taken from the plane of interest with a pulse separation of 1 msec. A BNC 565 pulse-delay generator (Berkeley Nucleonics Corporation, Berkeley, CA) synchronizes the laser pump, high-speed camera, and the pulsatile pump at their proper frequencies such that the image acquisition is accurately triggered at the beginning of the cardiac cycle and imaging continued throughout several cardiac cycles.

An interrogation window of 32 × 32 pixels with 50% overlapping was found suitable for the current work according to the maximal displacement of the particles from one frame to another. Pixel dimensions were 0.0 5 × 0.05 mm². The velocity field was obtained by cross-correlating every two consecutive images with 1-msec pulse separation using PIVview2C (PIV TEC Gmbh, Göttingen, Germany). No averaging was made in obtaining the velocity frames. The imaging field of the aortic model in one of the experiments is illustrated in **Figure 2B**.

Postprocessing Analyses

Particle residence time. The time required for a designated particle to leave a region of interest (ROI) is defined as the particle residence time (T_p).[9] This index provides quantitative information about flow fields in certain regions around a heart valve and may correlate with perfusion limitation or enhancement when a transcatheter valve undergoes a change in position.[21] According to Kheradvar *et al.*,[9] T_p is calculated using equation 1 as:

$$T_p = \sum_{i=1} \frac{|\mathrm{D}x_i|}{|v_i|}, \quad \mathrm{D}x_i \pounds X \tag{1}$$

where x and v are displacement and velocity vectors for each particle in the flow-field, respectively. The number of frames that the particles were traced in the ROI is defined by the index *i*, and X is the dimensions of the area or ROI. To quantify flow stagnation created by each position of the transcatheter aortic valve, at the beginning of diastole, 1,000 virtual particles were randomly distributed in the ROI. Particles were then subjected to the acquired flow field and velocity field in each ROI as obtained using scattered data interpolation. The error of interpolation was approximated by:

$$|\mathrm{Err}| = \left|u_i - u_{i_{\mathrm{int}}}\right| \le \frac{1}{4} M_2 h^2 + \frac{1}{64} M_4 h^4 \tag{2}$$

where *i* represents either *u*- or *v*-component of the velocity, h = max ($\Delta x, \Delta y$), M_2 = max($|\partial^2 u_f/\partial x^2|$, $|\partial^2 u_f/\partial y^2|$), and M_4 = max($|\partial^4 u_f/\partial x^2 \partial y^2|$). Using the interpolated velocity vectors and the time gap between each frame, the displacement vector for each particle at each time instant was calculated. The displacement vectors were used to update the new location for the particle until the particle moved out of the ROI, at which time it was considered a washed-away particle.

Reynolds shear and normal stresses. Reynolds stresses have recently attracted much attention and provide useful information regarding blood cell damage. The Reynolds shear stress has also been frequently used as equivalent to the viscous shear. In our work, since the flow downstream of the TAVR had a high fluctuation in the velocity field, we chose Reynolds stresses to quantify the stresses due to randomness and fluctuation of the flow when we implanted the TAVR.

Reynolds shear stress is quantified based on the velocity fields obtained by DPIV analysis. The magnitude and symmetry of the shear stress can have significant effects on the wall of the aorta and the aortic valve leaflets.[22,23] Since Reynolds stresses are not invariant under coordinate rotation, the stresses were calculated along the principal stress axes. Shear stress $\left(\overline{\rho uv}\right)$ was computed in one cardiac cycle according to equations 3 to 5:

$$\overline{\rho uu} = \frac{1}{N}\sum_{t=1}^{N} \rho u'^2 \tag{3}$$

$$\overline{\rho vv} = \frac{1}{N}\sum_{t=1}^{N} \rho v'^2 \tag{4}$$

$$\overline{\rho uv} = \frac{1}{N}\sum_{t=1}^{N} \rho u'v' \tag{5}$$

where ρ is the density of the fluid, u' and v' are the components of the fluctuating velocity, and N is the number of velocity frames in one cycle. In the equations above, $\overline{\rho uu}$ and $\overline{\rho vv}$ are the Reynolds normal stresses, which are the stress components normal to the cross-section, and $\overline{\rho uv}$ representing Reynolds shear stress is the component parallel to the cross-section. This was accomplished by using the interpolated velocity vectors and the time gap between each frame, in order to calculate the displacement vector for each particle at each time instant. Displacement vectors were then used to update the new location for the particle until the particle moved out of the ROI, at which time it was considered a washed-away particle.

Data Analyses

For each position of the TAVR, the particle residence time and the Reynolds stresses were calculated. This computation was repeated for each cardiac output. The shear stresses are pertinent to determining the change in the cardiac flow field that occurs with a change in the position of the transcatheter valve. These factors illustrate how the forces on the valve leaflets and the aorta will change according to the valve position. The particle residence time in sinuses of Valsalva can directly influence local vascular perfusion that primarily occurs during diastole.[7,21] Through the application of fluid dynamics, the fundamental principles for each change in the flow resulting from each change in the placement of transcatheter valve can be determined.

Postprocessing

The transcatheter valve was positioned within the aortic valve at four different distances from the valve annulus. Each position was analyzed at two different states of cardiac output.

Combining the four valve positions tested at each cardiac output, we arrived at eight distinct data sets. Particle residence time was calculated for a population of 1,000 particles and then plotted as a function of the valve position with respect to the annulus for 2 and 4 L/min of cardiac output. Through this comparison, the relative valve positions were compared at each distinct cardiac output. In addition, the T_p data set was broken down by the percentage of particles that remained in the regions of interest for predefined time periods to reach the final T_p. With respect to the normal and shear stress values, a representation of the magnitude and symmetry of the stress was plotted over the aortic model and illustrated for direct comparison.

Results

The sinus of Valsalva in our aortic model was targeted for as the region of interest. For every valve position and flow rate, particle residence time at the sinus and Reynolds shear stresses within the aortic chamber were calculated. The residence time was calculated for a distribution of 1,000 imaginary particles for each valve, which gives a large enough sample size to accurately determine the effect of the change in valve position.

Particle Residence Time

Figure 3 is a graph of the change in the average particle residence time that occurs according to the valve position with respect to the bioprosthetic aortic valve annulus. The two plotted series represent the changes that occur at the two different flow rates at which the experimental conditions were replicated (stroke volume of 33 and 66 mL, respectively). Since the experimental conditions for the two valves were identical, the results produced for particle residence time were consistent; this can be seen in **Table 1**. With a heart rate of 60 bpm, the cardiac output was first set at 2 L/min to represent a low-output state and then at 4 L/min (stroke volume 33 and 66 ml). Previous work has shown that changes in the heart rate do not produce significant changes in *in vitro* simulations over a range of 50–90 bpm with regard to hemodynamics; but changes in cardiac output do produce measurable changes.[24] Cardiac output settings were chosen due to the replication of two states of the LV function: a low-output state, and a near-normal state with a normal stroke volume.

In **Figure 3**, it is illustrated that at a flow rate of 2 L/min the particle residence time remains constant across the first two valve positions at about 0.5 sec; however, when the valve was displaced from the annulus to 15 mm and then to 20 mm, the particle residence time decreased to 0.42 sec and then to 0.38 sec. Once the flow rate was increased to 4 L/min a substantially different pattern was observed in the particle residence time. At valve positions of 5 and 20 mm from the annulus, (i.e., the extremes of the experimental design), the particle residence times were 0.43 and 0.5 sec, respectively. However, in the intermediate positions of 10 and 15 mm, the particle residence times dramatically decreased to 0.1 and 0.16 sec, which are only 10 and 16% of the cardiac cycle, respectively. It should be noted that the error produced by interpolation for both *u*- and *v*-component of the velocity was negligible and was found to be in the order of 10^{-6} for all the cases.

These data come with the caveat that particle residence time is indicative of the time it takes for the particles to be completely washed out of the sinus. In **Figure 4**, we have shown the breakdown of the percent of particles that were washed out in time within the sinus at various time points. For a valve position of 5 mm below the annulus, at a flow rate of 4 L/min, the vast majority of the particles are in fact washed out by 0.3 sec and only a few remain past that time. For a valve position of 20 mm, nearly 90% of the particles are washed out by 0.2 sec and very few lasted past 0.3 sec.

Aortic Reynolds' Normal and Shear Stress

The Reynolds' normal and shear stresses downstream of the transcatheter aortic valve are also major concerns for the placement of a transcatheter valve. With a change in the flow patterns that result from a change in the position of the valve annulus, there is a change in the normal and shear stresses in the aorta. To determine this we have computed both the normal and shear stresses in the aorta model. This is shown in **Figures 5** and **6** where the shear stresses are plotted. Normal stresses followed a very similar pattern and are not included. Here it can be seen that at the lower flow rate, the shear and normal stresses are relatively low and the change among valve positions is not dramatic. However, the one exception to this is the valve that was positioned 10 mm from the annulus, which showed an increase in both shear and normal stresses.

When the flow rate increased to 4 L/min, which is a better representative of the normal state of cardiac function, the Reynolds' normal and shear stresses dramatically changed. **Figure 6D** shows that at a displacement of 20 mm the intensity

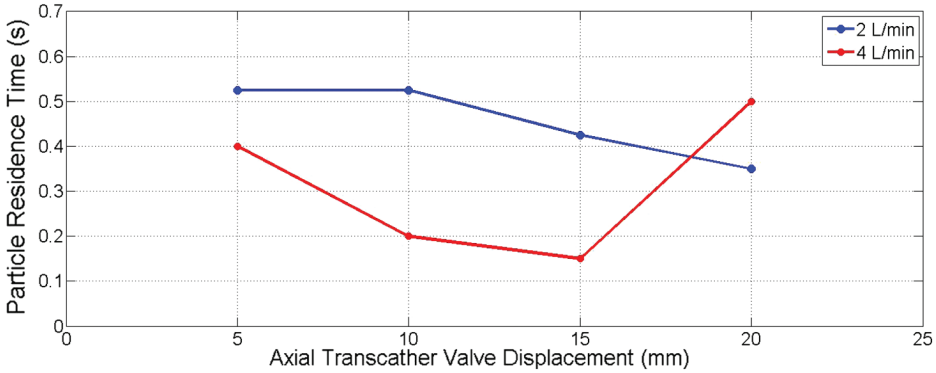

Figure 3. Graph of valve position with reference to the native annulus *versus* particle residence time for the two distinct states of cardiac output. full color online

Table 1. Comparison of the Particle Residence Times for the Two Transcatheter Valves Examined

		Displacement (mm)			
CO (L/min)	Valve, No.	5, sec	10, sec	15, sec	20, sec
2	1	0.53	0.54	0.42	0.38
	2	0.56	0.57	0.44	0.40
4	1	0.43	0.1	0.16	0.5
	2	0.37	0.3	0.14	0.5

Results were similar and consistent. All the virtual particles were washed away in less than the duration of a cardiac cycle for both valves.

CO, cardiac output.

of both normal and shear stresses have become more prominent on the wall of aorta.

Discussion

Transcatheter aortic valve replacement is a revolutionary technology with a potential to be more commonly used in the near future. A critical component of the procedure is precise valve placement. Through this work, we have used a series of *in vitro* experiments using an advanced left heart flow simulator to study the hemodynamic effects of varying valve position.[25–27] Hemodynamics of valve placement are especially relevant with respect to coronary perfusion and the stress exerted along the wall of the aorta.[27]

Effects of Positioning on Aortic Root Residence Time and Coronary Perfusion

The results of our experiments indicate that at a state of low cardiac output, the particles remained in the sinus of Valsalva for a constant period of time at 5 and 10 mm displacement with respect to the aortic annulus. Residence time then diminished with increasing annular displacement, until the nadir at a displacement of 20 mm. These results are consistent with the hemodynamics of a low-output state; given a low flow rate with constant area, flow velocities are reduced significantly, and, thus, the washout of the particles is less affected. Moreover, the residence time is preserved for the majority of valve positions with the exception of the displacement by 20 mm, which is possibly too dramatic a shift in the position of the transcatheter valve with respect to aortic anatomy to maintain proper perfusion.

By increasing the cardiac output, particle residence time remained optimal at both 5- and 20-mm positions. All particle residence times were less than 1 sec, which was the length of the cardiac cycle in the experiment. This indicates that there is minimal risk of thrombosis; however, if the particle residence time is too short, there may be negative consequences on coronary perfusion.

Although similar numerical values for the particle residence time at both 5- and 20-mm valve positions were found, these two values represent quite different particle retention within the sinus and, perhaps, may exert different effects on coronary perfusion.

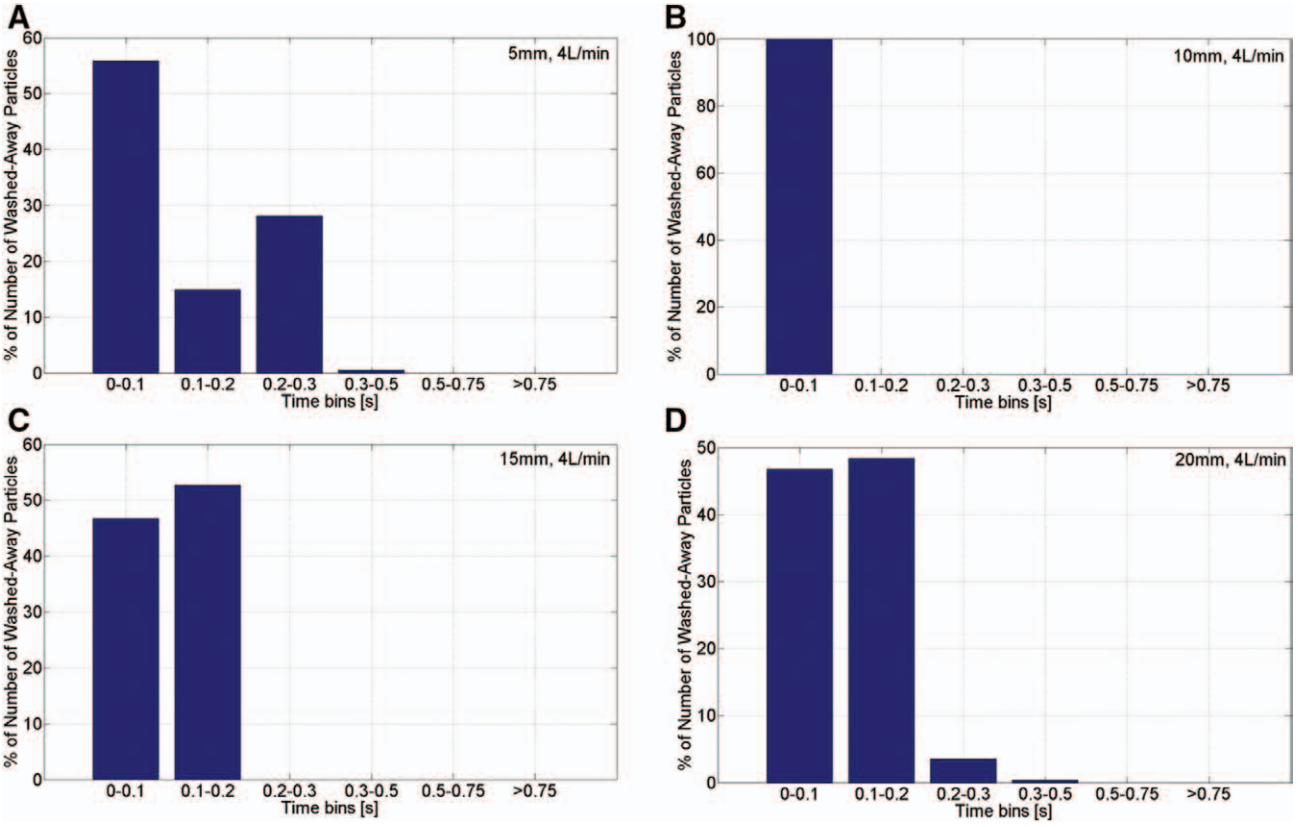

Figure 4. Representation of particle residence time at 4 L/min of cardiac output based on the percent of particles washed out of sinus of Valsalva (region of interest) at each distinct time interval. For each time interval a certain portion of particles are washed out. (**A**) 5-mm displacement, (**B**) 10-mm displacement, (**C**) 15-mm displacement, and (**D**) 20-mm displacement. It can be observed that a far greater percent of the particles remain in the sinus past 0.2 sec in the 5-mm displacement than in the 20-mm displacement. full color online

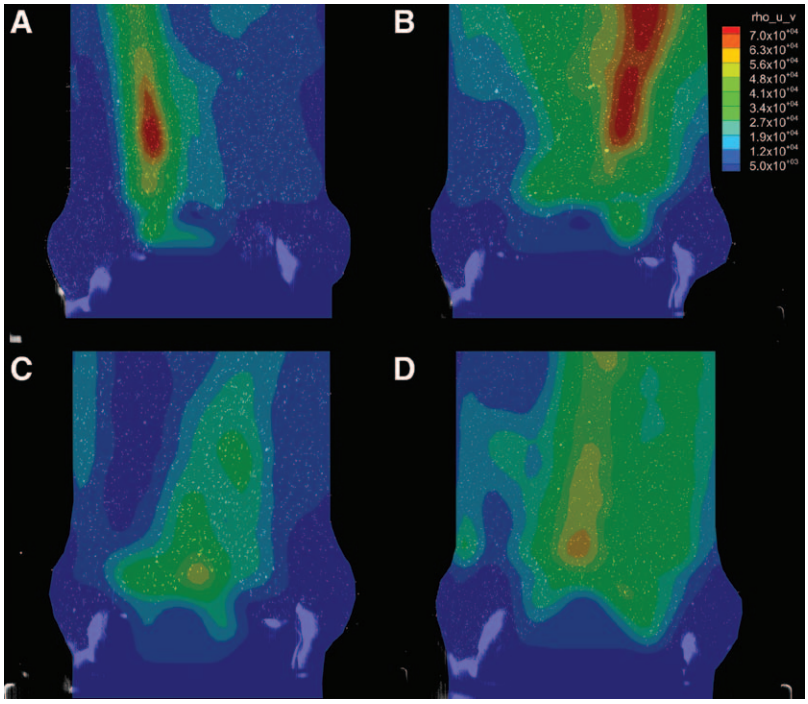

Figure 5. Reynolds' shear stress at 2 L/min of cardiac output. Magnitude of the shear stress is indicated in the following color scheme: Blue indicates low values, and the colors green, yellow, orange, and red indicate increasing values. (**A**) 5-mm displacement, (**B**) 10-mm displacement, (**C**) 15-mm displacement, and (**D**) 20-mm displacement. For all values other than 10-mm displacement, the stress distribution is relatively low and symmetric. full color online

The reason the numerically identical values are not equivalent is that different factors can influence the particle residence time. At 20 mm of displacement and with 4 L/min of cardiac output, substantial paravalvular leak was observed due to suboptimal positioning, which in turn artificially bolsters the particle residence time but can be deleterious to the patients' left ventricle.

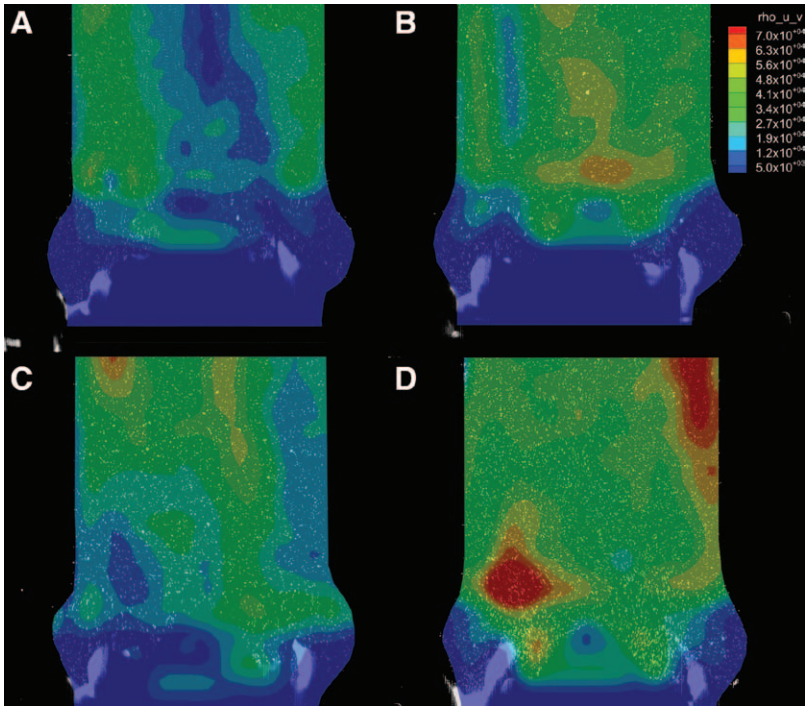

Figure 6. Reynolds' shear stress at 4 L/min of cardiac output. Magnitude of the shear stress is indicated in the following color scheme: Blue indicates low values, and the colors green, yellow, orange, and red indicate increasing values. (**A**) 5-mm displacement, (**B**) 10-mm displacement, (**C**) 15-mm displacement, and (**D**) 20-mm displacement. With an increase in displacement, the shear stress increases dramatically and becomes more unstable and asymmetric. full color online

The fact that the 5-mm displacement did not include that caveat and a large portion of the particles persisted in the sinus may suggest that this position is associated with an optimal particle residence time. This would in turn indicate that the placement of the transcatheter valve very close to the native annulus (*i.e.*, no more than 5-mm displacement) is perhaps an ideal position.

Aortic Wall Stresses

Further examination of the effects of the transcatheter valve's positioning included studying the effects on the Reynolds' normal and shear stresses in the aorta. It has been well documented that an increase in aortic stress and an asymmetry in that stress as a result of AS can cause a poststenotic dilation.[22] This is a result of the asymmetry of the distribution of the Reynolds' normal and shear stresses, along with an increase in their magnitudes. From a clinical perspective, increasing magnitudes of wall stresses may result in damage to blood components and potential aortic wall rupture or dissection. Therefore, the stress distributions of the various valve positions were studied to determine whether there was a significant change produced by displacement of the transcatheter valve from the native annulus.

Shear stresses are represented in **Figures 5** and **6**. As can be seen, there is no substantial change in the magnitude or symmetry of the stresses at the low-cardiac-output setting until the valve is displaced to 10 mm, where there is a minor increase in magnitude. However, once the cardiac output was increased, there was a substantial change in both the Reynolds' normal and shear stresses for all the valve positions. A position of 5 mm below the annulus produced a low and symmetrically distributed stress profile. Once the valve was further displaced, the Reynolds' normal and shear stresses steadily increased and became more asymmetric. This increase and asymmetry could mimic the pathologic conditions associated with AS and, thus, may impose deleterious effects on the aorta.[22] In addition, the lifespan of pericardial tissue leaflets is limited under normal conditions; if there is increased stress exerted upon them, this limited lifespan may be even further shortened.

As we increased the cardiac output and stroke volume, the valve positioned 5 mm from the native annulus continued to have Reynolds' shear stresses, which were symmetrical and of low intensity. This is perhaps consistent with the normal and shear stresses produced in the aorta by the blood flow through a nondiseased native aortic valve. However, unlike in the low-cardiac-output state, where significant displacement was required to alter the stresses, here, as the valve displacement from the native annulus increased, the stresses within the aorta immediately became more asymmetric and considerably increased. Thus, as the cardiac output and stroke volume increase, the asymmetry of the stresses are substantially more influenced by the valve position and may have an even greater negative effect on valve function and durability.

Clinical Impact

By utilizing a carefully designed series of *in vitro* experiments, we have studied the hemodynamic consequences of various positions of a transcatheter aortic valve placement. These experiments demonstrated that placement of the transcatheter valve annulus should be carefully matched to be at or just below the aortic valve annulus.

From a clinical perspective, these studies highlight the need for increased accuracy in procedural imaging to accurately implant TAVR devices within either the native aortic or a previously implanted annulus. Currently, catheterization labs rely largely upon angiography to position the prosthetic valve. However, this two-dimensional imaging modality may not be sufficient to properly place the valve in the optimal position. Further research is required to investigate new procedural imaging techniques that may improve outcomes. Additional clinical implications include the potential advantages of using a repositionable valve, including, importantly, the overall risk mitigation facilitated by such a valve. Finally, making clinicians aware of the potential consequences of increased annular displacement may foster the development of more accurate delivery systems. A weakness of our study is that we did not directly simulate the coronary perfusion. We focused only on the hemodynamics downstream of the TAVR valve; as a result, we did not have the upstream velocity field. Therefore, we are unable to estimate the pressure gradient and energy loss.

Conclusion

In summary, valvular hemodynamics is an important consideration in TAVR as long-term outcomes may be substantially affected if the flow is altered through a transcatheter valve. Both particle residence time and Reynolds' shear stress downstream of the transcatheter valve were substantially affected by the position of a valve in our experiments. We have shown that placement of a transcatheter valve within the annulus of a bioprosthetic valve at no more than 5-mm distance from the annulus should be ideal. Any further displacement of the valve can be associated with detrimental effects on the observed hemodynamics. The study results suggest that the transcatheter valve placement as close to the native valve annulus as possible will provide optimal hemodynamics in the sinuses of Valsalva and ascending aorta.

Acknowledgments

The authors thank Folda, LLC, for providing the transcatheter aortic valve, and Edwards Lifesciences (Irvine, California) for providing the bioprosthetic aortic valves used in this study.

References

1. Dewey TM, Brown D, Ryan WH, Herbert MA, Prince SL, Mack MJ: Reliability of risk algorithms in predicting early and late operative outcomes in high-risk patients undergoing aortic valve replacement. *J Thorac Cardiovasc Surg* 135: 180–187, 2008.
2. Holmes DR Jr, Mack MJ, Kaul S, *et al*: 2012 ACCF/AATS/SCAI/STS expert consensus document on transcatheter aortic valve replacement. *J Am Coll Cardiol* 59: 1200–1254, 2012.
3. Luo Z, Cai J, Gu L: A pilot study on magnetic navigation for transcatheter aortic valve implantation using dynamic aortic model and us image guidance. *Int J Comput Assist Radiol Surg* 8: 677–690, 2013.
4. Al-Attar N, Ghodbane W, Himbert D, *et al*: Unexpected complications of transapical aortic valve implantation. *Ann Thorac Surg* 88: 90–94, 2009.
5. Leipsic J, Gurvitch R, Labounty TM, *et al*: Multidetector computed tomography in transcatheter aortic valve implantation. *JACC Cardiovasc Imaging* 4: 416–429, 2011.
6. Willson A, Toggweiler S, Webb JG: Transfemoral aortic valve replacement with the SAPIEN XT valve: Step-by-step. *Semin Thorac Cardiovasc Surg* 23: 51–54, 2011.

7. Anayiotos AS, Pedroso PD, Eleftheriou EC, Venugopalan R, Holman WL: Effect of a flow-streamlining implant at the distal anastomosis of a coronary artery bypass graft. *Ann Biomed Eng* 30: 917–926, 2002.
8. Shi Y, Yeo TJ, Zhao Y, Hwang NH: Particle image velocimetry study of pulsatile flow in bi-leaflet mechanical heart valves with image compensation method. *J Biol Phys* 32: 531–551, 2006.
9. Kheradvar A, Kasalko J, Johnson D, Gharib M: An *in vitro* study of changing profile heights in mitral bioprostheses and their influence on flow. *ASAIO J* 52: 34–38, 2006.
10. Saikrishnan N, Yap CH, Milligan NC, Vasilyev NV, Yoganathan AP: *In vitro* characterization of bicuspid aortic valve hemodynamics using particle image velocimetry. *Ann Biomed Eng* 40: 1760–1775, 2012.
11. Wendt D, Stühle S, Piotrowski JA, *et al*: Comparison of flow dynamics of Perimount Magna and Magna Ease aortic valve prostheses. *Biomed Tech (Berl)* 57: 97–106, 2012.
12. Falahapisheh A, Kheradvar A: High-speed particle image velocimetry to assess cardiac fluid dynamics *in vitro*: From performance to validation. *Eur J Mech B Fluids* 35: 2–8, 2012.
13. Chi-Wen L, Sheng-Fu C, Chi-Pei L, Po-Chien L: Cavitation phenomena in mechanical heart valves: Studied by using a physical impinging rod system. *Annals of Biomedical Engineering* 38: 3162–3172, 2010.
14. Lee H, Tatsumi E, Taenaka Y: Flow visualization of a monoleaflet and bileaflet mechanical heart valve in a pneumatic ventricular assist device using a PIV system. *ASAIO J* 56: 186–193, 2010.
15. Stühle S, Wendt D, Houl G, *et al*: *In-vitro* investigation of the hemodynamics of the Edwards Sapien transcatheter heart valve. *J Heart Valve Dis* 20: 53–63, 2011.
16. Heart A: Development and evaluation of a novel artificial catheter-deliverable prosthetic heart valve and method for *in vitro* testing. *Int J Artif Organs* 32: 262–271, 2009.
17. Roman MJ, Devereux RB, Kramer-Fox R, O'Loughlin J: Two-dimensional echocardiographic aortic root dimensions in normal children and adults. *Am J Cardiol* 64: 507–512, 1989.
18. Tamborini G, Galli CA, Maltagliati A, *et al*: Comparison of feasibility and accuracy of transthoracic echocardiography *versus* computed tomography in patients with known ascending aortic aneurysm. *Am J Cardiol* 98: 966–969, 2006.
19. Maeda K, Kuratani T, Torikai K, *et al*: Impact of electrocardiogram-gated multi-slice computed tomography-based aortic annular measurement in the evaluation of paravalvular leakage following transcatheter aortic valve replacement: The efficacy of the OverSized AortiC Annular ratio (OSACA ratio) in TAVR. *J Card Surg* 28: 373–379, 2013.
20. Bjursten H, Götberg M, Harnek J, Nozohoor S: Successful transcatheter valve-in-valve implantation in a small deteriorated aortic valve bioprosthesis. *J Heart Valve Dis* 22: 433–435, 2013.
21. White SS, Zarins CK, Giddens DP, *et al*: Hemodynamic patterns in two models of end-to-side vascular graft anastomoses: Effects of pulsatility, flow division, Reynolds number, and hood length. *J Biomech Eng* 115: 104–111, 1993.
22. Wilton E, Jahangiri M: Post-stenotic aortic dilatation. *J Cardiothorac Surg* 1: 7, 2006.
23. Yap CH, Saikrishnan N, Tamilselvan G, Yoganathan AP: Experimental technique of measuring dynamic fluid shear stress on the aortic surface of the aortic valve leaflet. *J Biomech Eng* 133: 061007, 2011.
24. Yap CH, Saikrishnan N, Tamilselvan G, Yoganathan AP: Experimental measurement of dynamic fluid shear stress on the aortic surface of the aortic valve leaflet. *Biomech Model Mechanobiol* 11: 171–182, 2012.
25. Al Ali AM, Altwegg L, Horlick EM, *et al*: Prevention and management of transcatheter balloon-expandable aortic valve malposition. *Catheter Cardiovasc Interv* 72: 573–578, 2008.
26. von Segesser LK, Gerosa G, Borger MA, Ferrari E: Prevention and management of potential adverse events during transapical aortic valve replacement. *J Heart Valve Dis* 22: 276–286, 2013.
27. Wang Q, Sirois E, Sun W: Patient-specific modeling of biomechanical interaction in transcatheter aortic valve deployment. *J Biomech* 45: 1965–1971, 2012.